

EFFECTS OF BUILDING INTERFERENCE ON A GENERIC BUILDING MODEL

Abdul Hafiz Azizan^{1*} and Shabudin Mat^{1,2}

¹Faculty of Mechanical Engineering, Universiti Teknologi Malaysia, 81310 UTM Johor Bahru, Johor, Malaysia

²UTM Aerolab, Institute for Vehicle Systems & Engineering, Universiti Teknologi Malaysia, 81310 UTM Johor Bahru, Johor, Malaysia

Article history

Received

21st February 2024

Received in revised form

2nd May 2024

Accepted

8th April 2024

Published

1st June 2024

*Corresponding author

abdul.hafiz@graduate.utm.my

ABSTRACT

The presence of nearby buildings would alter wind flow patterns around the existing building and may lead to interference effects. In previous studies, detailed explanations on the interference effects between buildings are not well explained. Thus, the purpose of this study is to investigate the interference effect, particularly the effect of different height ratios of the interfering building and different wind incident angles. The experiment was conducted in the UTM-LST wind tunnel where surface pressure was measured on both of the wall and the roof of the target building of a generic building model. Based on the result obtained, the interference factor, IF for the South Wall B were 0.9, 0.6, and 0.2 for interference height 0.3H, 0.6H, and H respectively. These values represent a reduction of wind load on the building façade where the highest was an 80% reduction. On the roof, the IF obtained were 1.4, 0.9, and -0.2 for interference heights of 0.3H, 0.6H, and H respectively. The suction load was increased by 40% for interference height of 0.3H and decreased by 20% and 120% for interference height of 0.6H and H.

increasing intensity of these buildings have altered the wind flow patterns around them. These changes in wind flow patterns around buildings could produce shielding effect in which reduces wind load on downstream buildings and amplification effect where it can lead to major issues such as structural failures and disturbances in pedestrian wind comfort. The effects are commonly known as the interference effect between buildings.

The flow of air around areas with high-intensity and tall buildings is more complex compared to isolated buildings. Consequently, a substantial amount of research has been conducted in the field of wind engineering, with the interference effect between buildings being one of the prominent areas of study. Most of the studies have focused on three main topics which were wind loads [1, 2, 6], wall cladding design [3, 4], and pedestrian-level wind comfort [11]. Various parameters, including geometrical factors [1, 2, 5, 7, 10], distances between buildings [4, 7, 8, 10], building arrangements [2, 4, 9], wind direction [4], [7], and upstream terrain condition [6], have been evaluated in previous studies to understand the interference effects between buildings. Wind loads, surface pressure, and wind velocity around downstream buildings have been measured to study the shielding and amplification effects. These effects commonly were evaluated using interference factor (IF) [2]. The definition of this parameter was depended on the quantities being measured such as aerodynamic forces [9, 10], and wall cladding pressure [7, 8].

However, most of these studies were conducted on simple building designs, especially square and rectangular structures. Additionally, most of them only considered the interference effect between two buildings. In reality, buildings often have irregular shapes and are surrounded by

KEYWORDS

Wind tunnel test; Interference effects; Irregular building

INTRODUCTION

The increasing number of human populations has led to the construction of more buildings over the years. Different geometrical sizes and shapes with

complex arrangements. Thus, translating research findings to the real world could be difficult. In terms of interference effects on building roofs, there are relatively few studies available. Significant result from these studies have indicated that both shielding and amplification effects can occur on roofs due to interference effects. However, these studies mostly focused on the impact of low-rise buildings of similar sizes and the effect of high-rise buildings on low-rise structures [12, 13]. Further research is needed to evaluate the effect of smaller interfering buildings.

As the interference effect between buildings was not clearly explained in previous work. Therefore, the purpose of this study is to investigate interference effects, particularly focusing on the impact of different height ratios of interfering buildings and various wind incident angles.

METHODOLOGY

In this study, a generic building model was used to investigate interference effects. The model consists of one main building surrounded by several smaller structures. The primary focus was on the main building with dimensions of 220 mm in width, 245 mm in length, and 392 mm in height, serving as the target structure. In the direction of the wind flow, a small shed roof building was situated upstream, with a conical structure located to the right. Figure 1 provides further details on this model. To facilitate surface pressure measurements, 29 pressure taps were installed on the windward wall (South Walls A and B) and the roof area of the main building, as shown in Figure 2.

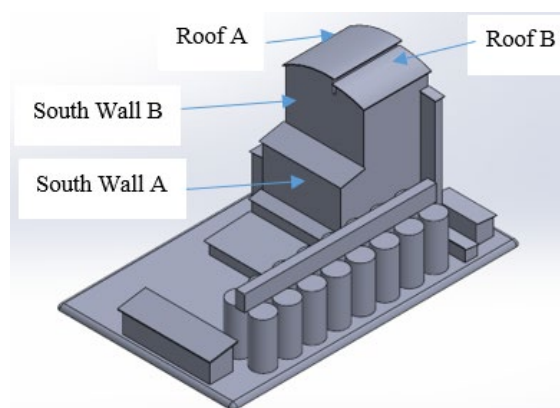


Figure 1: Generic building model

For the study's purposes, three different heights of interfering building models were fabricated. The plan dimensions of these models were similar in

size to the target building in the UTM generic building model, with a width and length of 220 mm and 245 mm, respectively. The heights of these interfering buildings were set at 0.3H, 0.6H, and H, where H represents the height of the target building which is 392 mm.

Both the principal and interfering buildings were placed on the turntable in the test section of the UTM-LST wind tunnel. The interfering building was positioned upstream of the incoming flow as depicted in Figure 3. In each configuration test, the distance between the interfering building and the lower wall of the target model was fixed at 3.4D. This distance corresponds to the space between the centre of the UTM building model and the centre of the interfering building models.

Surface pressure measurements were conducted on South Wall A and South Wall B of the south wall, and both Roof A and Roof B of the roof, using a static pressure taps system. An automatic FKPS 30DP electronic pressure scanner with an accuracy of ± 1 psi was used to measure the pressures. As the FKPS 30DP has 30 pressure ports, only 29 pressure taps were utilized for the surface pressure measurement, with the remaining one used to measure the static pressure of the upstream velocity.

For data acquisition and control, the FKPS 30DP electronic pressure scanner was connected to a data acquisition system operated using LABVIEW software. During the experiment, measurements were taken at a rate of 1000 Hz per sample, resulting in ten samples and a total of 10,000 pressure data points for each pressure tap at a given wind incident angle. At the start of the experiment, tare measurements for each pressure tap were performed at a wind incident of 0° and a wind speed of 0 m/s. Subsequently, pressure measurements were carried out at various wind incident angles ranging from -30° to 30° in 10° increments, with a wind speed of 12 m/s. These pressure measurements were repeated for two additional building configurations at the same wind speed. Due to the limited number of pressure taps, surface pressure on the roof of the UTM generic model was measured separately using the same procedure.

From the surface pressure measurements, mean pressure coefficients were calculated using the following relations:

$$C_p = \frac{p - p_\infty}{\frac{1}{2} \rho V_\infty^2} \quad (1)$$

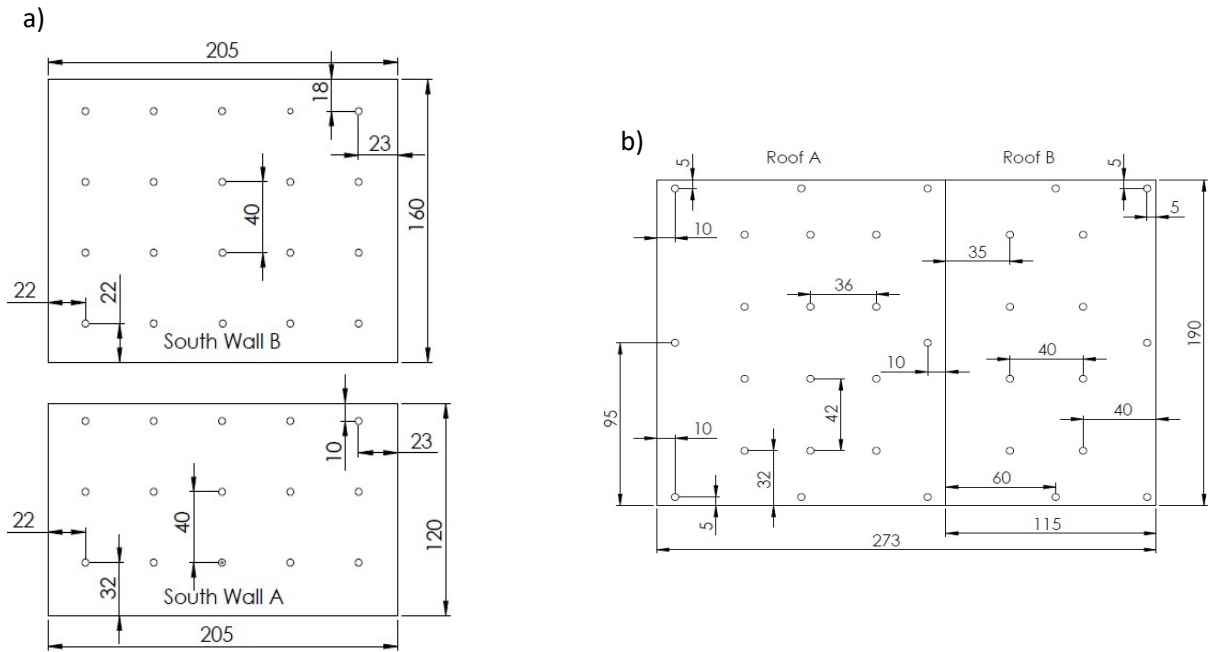


Figure 2: Pressure taps location. (a) Windward wall and (b) Roof

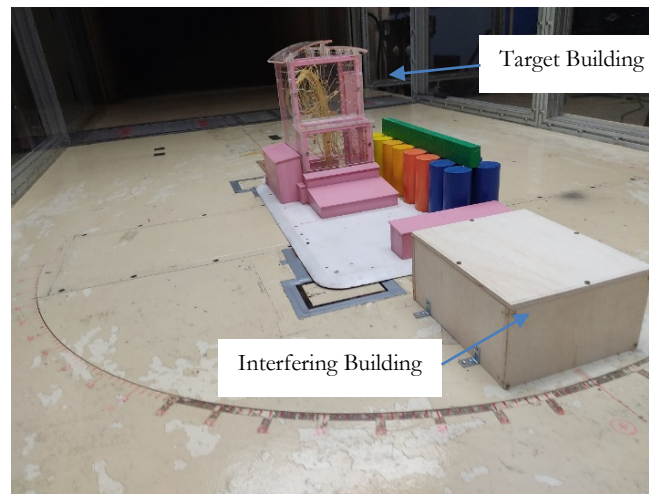


Figure 3: Test configuration in wind tunnel test section

Where, C_p represents the coefficient of pressure, p is the mean static pressure, p_∞ is the free stream static pressure, ρ is the density of the air, and V_∞ is the stream velocity.

The average weighted area pressure coefficient was determined using this formula:

$$C_{p,face} = \frac{\sum_{i=1}^n (C_{p,i} \times A_i)}{\sum_{i=1}^n A_i} \quad (2)$$

Where, $C_{p,face}$ is the area weighted average mean pressure coefficient, $C_{p,i}$ is the pressure coefficient

as specific pressure taps location, A_i is the area on specific surface of the target building.

The interference effect was evaluated using this relation:

$$\text{Interference Factor, } IF = \frac{C_{p,face} \text{ max(with interfering building)}}{C_{p,face} \text{ max (without interfering building)}} \quad (3)$$

Where, IF is the interference factor, $C_{p,face} \text{ max}$ is the maximum area weighted average mean pressure coefficient.

RESULTS AND DISCUSSIONS

No interference conditions

For no interference condition, results of pressure distribution contour plots for both South Wall A and South Wall B as shown in Figure 4 shows positive pressure due to direct impact from the wind flow. However, the results obtained were not symmetry as commonly found in literature due to the existing structure on the right side of the target building model. The effect of this structure more dominant on South Wall A as pressure

coefficient on the half of the right area was significantly reduced. The effect of insufficient numbers of pressure taps also observed at the South Wall A in which had affected the result.

Negative pressure coefficient was observed on both Roof A and Roof B at windward area of the roof as shown in Figure 5. At certain area, the value of the pressure coefficient was become zero. These variation of pressure coefficients was believed to have relation to the flow separation and reattachment that occur on the both roofs. For the roof B the result also was affected by the insufficient number of pressure taps.

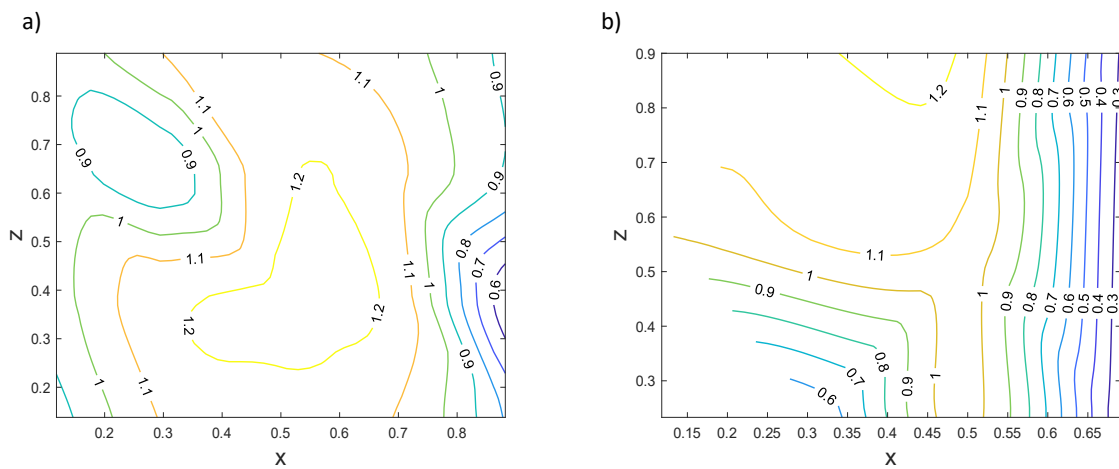


Figure 4: Mean pressure coefficients plot at $\alpha = 0^\circ$. a) South Wall B, b) South Wall A

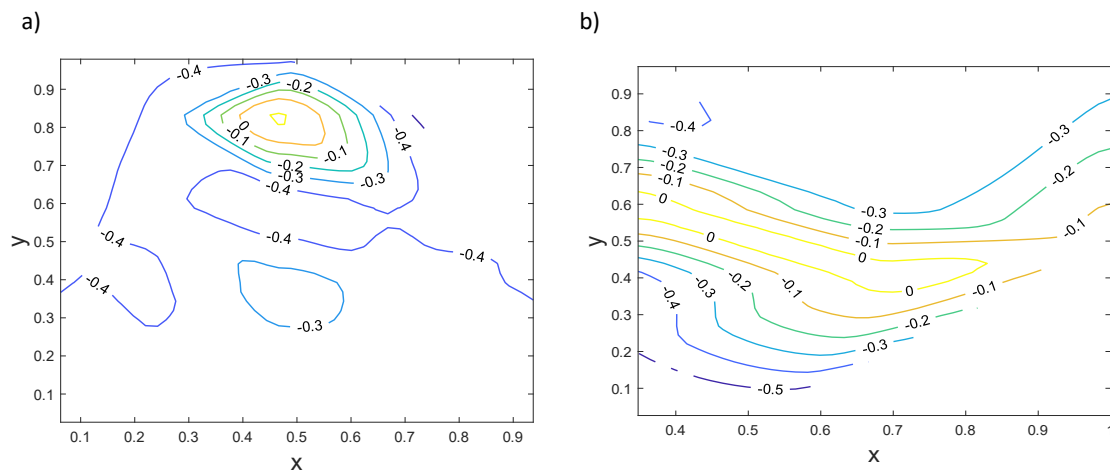


Figure 5: Mean pressure coefficients plot at $\alpha = 0^\circ$. a) Roof A, b) Roof B

Presence of the interfering buildings

For the interference effect of an upstream building, shielding effect was observed where the pressure coefficients on the South Wall B significantly reduced as the height of the interfering building increased. Meanwhile both amplification effect and shielding effect was observed on the roof of the target building. Higher suction was observed at the windward area of the Roof A at interference height of 0.3H and 0.6H but vanished at H. The trend of these amplification and shielding effect was clearly observed from mean pressure distribution along centre line plot for both wall and roof as shown in Figure 6 and Figure 7. The mixed effects observed on the roof area as obtained in Figure 7 might be related to the vortex shedding effects from the upstream interfering building.

The relation of interference heights and wind directions was established using weighted area pressure coefficient plot. The result had shown that the interference effect of all different interfering heights was highest at wind incident of 0° for buildings in tandem arrangement as shown in Figure 8 and Figure 9.

Lastly, the inference effect was evaluated in term of interference factor, IF. On the South Wall B, IF obtained were 0.9, 0.6 and 0.2 for interference height 0.3H, 0.6H and H respectively. These values represent reduction of wind load on the building façade where the highest was 80% of reduction. On the roof, the IF obtained were 1.4, 0.9 and -0.2 for interference height of 0.3H, 0.6H and H respectively. The suction load was increased 40% for interference height of 0.3H, and decreased 20% and 120% for interference height of 0.6H.

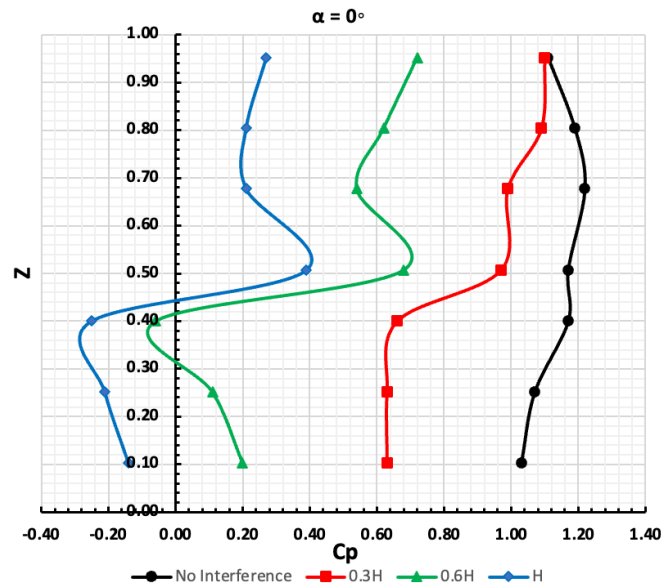


Figure 6: Mean pressure distribution along center line of the South Wall

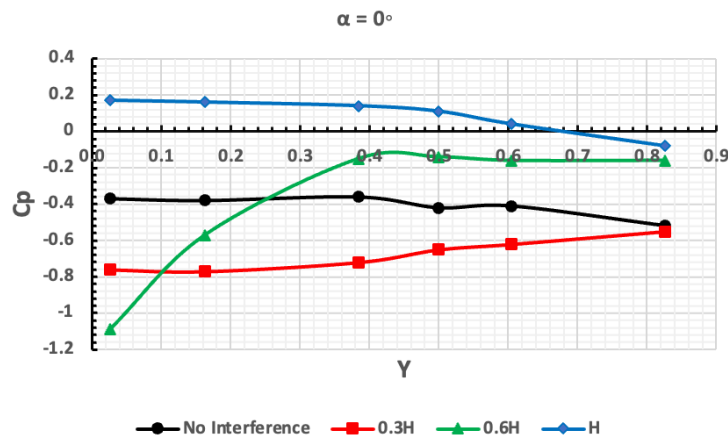


Figure 7: Mean pressure distribution along Roof A

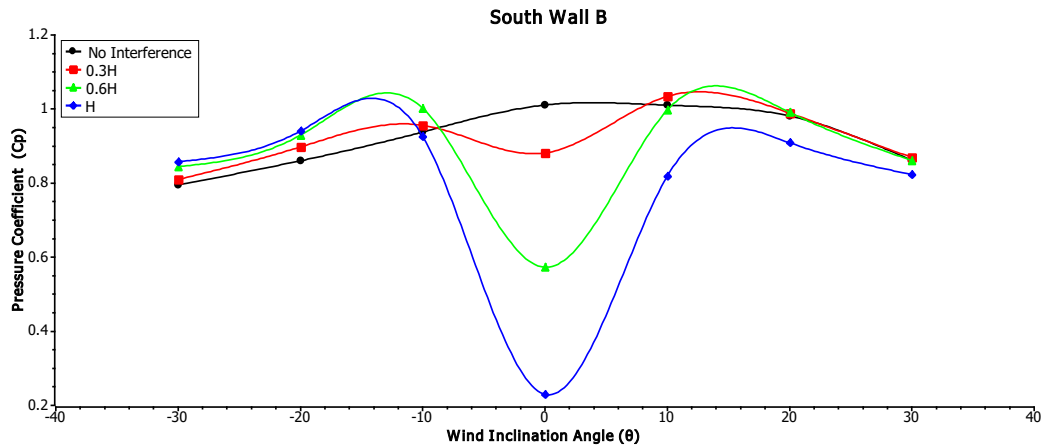


Figure 8: Weighted area average pressure coefficient of South Wall B

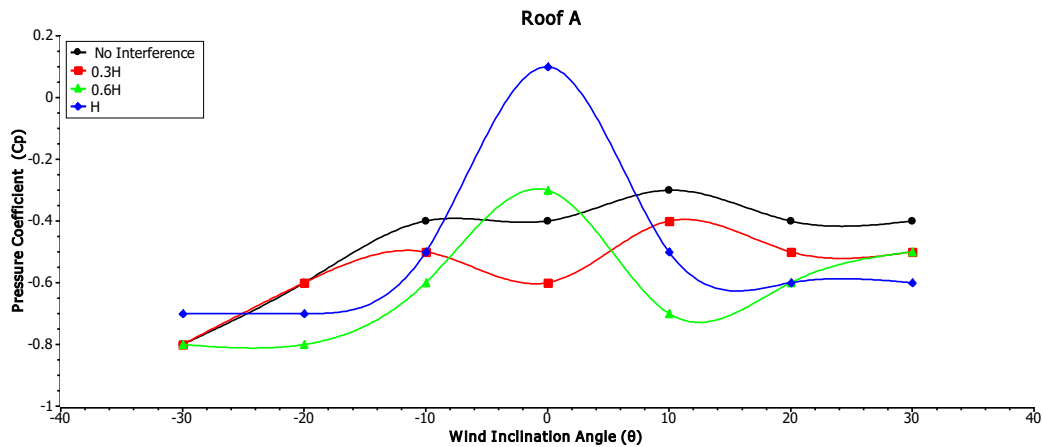


Figure 9: Weighted area average pressure coefficient of Roof A

CONCLUSION

The study on effect of different heights of interfering building and wind directions on the interference effects was conducted. Surface pressure measurement on generic building model was performed in UTM-LST wind tunnel. The results obtained had shown that presence of an upstream interfering building can provides shielding effect in which can reduce the wind load on the downstream building. At the same time, both shielding and amplification effect was observed at the roof area at certain conditions. Based on the interference factor, IF obtained, the highest reduction of mean pressure on the windward wall was 80%. While the highest amplification of the suction pressure at the roof was 40% and the highest reduction was 120%. For future improvements, flow visualization is recommended to understand details on the interference effects.

ACKNOWLEDGEMENT

This study was conducted at Universiti Teknologi Malaysia Aerolab using UTM-LST wind tunnel facility. Supports from Aerolab staffs are gratefully and acknowledged.

REFERENCES

- [1] Chauhan, B.S., Chakrabarti, A. and Ahuja, A.K., 2022, September. Study of wind loads on rectangular plan tall building under interference condition. In *Structures* (Vol. 43, pp. 105-130). Elsevier.
- [2] Kim, W., Tamura, Y. and Yoshida, A., 2015. Interference effects on aerodynamic wind forces between two buildings. *Journal of Wind Engineering and Industrial Aerodynamics*, 147, pp.186-201.
- [3] Hui, Y., Tamura, Y., Yoshida, A. and Kikuchi, H., 2013. Pressure and flow field investigation of interference effects on external pressures between high-rise buildings. *Journal of Wind Engineering and Industrial Aerodynamics*, 115, pp.150-161.

- [4] Hui, Y., Tamura, Y., Yoshida, A. and Kikuchi, H., 2013. Pressure and flow field investigation of interference effects on external pressures between high-rise buildings. *Journal of Wind Engineering and Industrial Aerodynamics*, 115, pp.150-161.
- [5] Yu, X.F., Xie, Z.N., Zhu, J.B. and Gu, M., 2015. Interference effects on wind pressure distribution between two high-rise buildings. *Journal of Wind Engineering and Industrial Aerodynamics*, 142, pp.188-197.
- [6] Mara, T.G., Terry, B.K., Ho, T.C.E. and Isyumov, N., 2014. Aerodynamic and peak response interference factors for an upstream square building of identical height. *Journal of Wind Engineering and Industrial Aerodynamics*, 133, pp.200-210.
- [7] Chen, B., Shang, L., Qin, M., Chen, X. and Yang, Q., 2018. Wind interference effects of high-rise building on low-rise building with flat roof. *Journal of Wind Engineering and Industrial Aerodynamics*, 183, pp.88-113.
- [8] Sy, L.D., Yamada, H. and Katsuchi, H., 2019. Interference effects of wind-over-top flow on high-rise buildings. *Journal of Wind Engineering and Industrial Aerodynamics*, 187, pp.85-96.
- [9] Zu, G.B. and Lam, K.M., 2018. Across-wind excitation mechanism for interference of twin tall buildings in staggered arrangement. *Journal of Wind Engineering and Industrial Aerodynamics*, 177, pp.167-185.
- [10] Chauhan, B.S., Chakrabarti, A. and Ahuja, A.K., 2021, June. Investigation of wind load alteration on rectangular cross-section tall building due to change in relative orientation of interfering building. In *Structures* (Vol. 31, pp. 970-981). Elsevier.
- [11] Tominaga, Y. and Shirzadi, M., 2021. Wind tunnel measurement of three-dimensional turbulent flow structures around a building group: Impact of high-rise buildings on pedestrian wind environment. *Building and Environment*, 206, p.108389.
- [12] Mohammad, A.F., Zaki, S.A., Ikegaya, N., Hagishima, A. and Ali, M.S.M., 2018. A new semi-empirical model for estimating the drag coefficient of the vertical random staggered arrays using LES. *Journal of Wind Engineering and Industrial Aerodynamics*, 180, pp.191-200.
- [13] H'ng, Y.M., Ikegaya, N., Zaki, S.A., Hagishima, A. and Mohammad, A.F., 2022. Wind-tunnel estimation of mean and turbulent wind speeds within canopy layer for urban campus. *Urban Climate*, 41, p.101064.